

Revisiting optical spectroscopy in a thin vapor cell: mixing of reflection and transmission as a Fabry–Perot microcavity effect

Gabriel Dutier, Solomon Saitiel, Daniel Bloch, and Martial Ducloy

Laboratoire de Physique des Lasers, Unité Mixte de Recherche 7538 du Centre National de la Recherche Scientifique, Université Paris 13, 99 Av J.-B. Clément, 93430 Villetaneuse, France

Received August 31, 2002; revised manuscript received December 12, 2002

Transmission spectroscopy in an ultrathin vapor cell, which has been recently demonstrated as a new method of sub-Doppler spectroscopy in the optical domain, is revisited. We show that, because of an unavoidable Fabry–Perot effect, the observed signal—in transmission spectroscopy and selective reflection spectroscopy as well—is actually an interferometric mixture of the optical responses as provided in transmission and in reflection by a long macroscopic cell. After the derivation of a very general solution, we restrict ourselves to the case of a linear interaction with the resonant laser. We finally discuss the application to a two-level atom for which analytical expressions are given, in the large Doppler limit, for FM transmission and reflection signals.

© 2003 Optical Society of America

OCIS codes: 300.6360, 120.2230, 020.1670, 020.3690.

1. INTRODUCTION

It has been recognized for some time that when selective reflection (SR) spectroscopy is performed under normal incidence at the interface between a transparent window and a resonant vapor, a sub-Doppler contribution is added to the usual dispersive spectrum.¹ The essential origin of this narrower response lies in the fact that, in spite of a resonant optical excitation, the atoms leave the surface of the window in the ground state and experience a transient interaction regime, so that only the slower atoms can reach the steady-state regime in the spatial region probed in SR spectroscopy. In optical transmission spectroscopy, a counterpart of this enhanced contribution of atoms with slow normal velocity can be found as long as the cell length is short enough,^{2–11} and the vapor dilute enough, so that atoms essentially fly wall to wall, their initial direction not being randomized by interatomic collisions. It is only recently that experimental evidence of this narrow contribution has been established with vapor cells whose minimal thickness ($\sim 10 \mu\text{m}$) was at least an order of magnitude larger than the optical wavelength.^{6–10} At the same time, theoretical models^{5,7} had also explained an enhanced contribution of slow atoms in transmission, along with the prediction of an interferometric behavior connected with the phase matching of the coherent buildup of the atomic response. In the experiments, an imperfect cell technology had hindered any possibility of observing interference effects^{7–9} that were, moreover, expected to be small for the relatively thick cells that were used. The further experimental development of cells whose thickness compares with the wavelength¹¹ implies that the window parallelism becomes intrinsically excellent, so that the multiple optical interference effects can no longer be neglected. For sake of simplicity, all of the previous models had also neglected the back reflection of the output window. It is the pur-

pose of this paper to provide an insight on the connection between the atomic absorption–dispersion response, and the monitored resonant line shapes at the transmission–reflection port of a Fabry–Perot (FP) type microcavity vapor cell.

Section 2 of the paper is very general and does not assume the slowly varying envelope approximation. It shows that the FP effect mixes, in a simple manner, the responses ordinarily connected with both transmission spectroscopy and SR spectroscopy. The derivation relies only on optical field propagation and is based simply upon the boundary conditions of the Maxwell equation. The derived solution does not make any assumption regarding the microscopic atomic response, which is supposed to be obtained independently. In subsequent parts, we go into more explicit expressions, discussing common approximations such as the optically thin medium (Section 3) and the linear regime of interaction with the driving field (Section 4) that make tractable the intrinsically coupled Maxwell–Schrödinger problem, mixing propagation and microscopic equations. We finally discuss an application of the derived calculations to the elementary case of a two-level atomic system that builds up coherently (Section 5), and give in Section 6 the corresponding analytical results in a FM spectroscopy approach.

2. REFLECTION AND TRANSMISSION OF A THIN FABRY–PEROT CELL FILLED WITH INHOMOGENEOUS, POLARIZED, DILUTED GAS

The problem that we consider is a pure one-dimensional problem, with diffraction and polarization effects neglected: A thin layer (thickness L) of an (resonant) atomic medium is sandwiched between two parallel dielectric windows assumed to be transparent (i.e., no ab-

sorptive or scattering losses) whose indices are n_1 for $z < 0$ and n_2 for $z > L$ (see Fig. 1). The medium is excited under normal incidence by an incident field $\mathbf{E}_{\text{in}}(z, t)$ propagating in the positive direction in the first window (n_1):

$$\mathbf{E}_{\text{in}}(z, t) = \frac{1}{2}E_{\text{in}} \exp[-i(\omega t - kn_1z)] + \text{c.c.} \quad (1)$$

In Eq. (1), ω is the circular frequency and k verifies $k = \omega/c$.

The purpose of the calculation is to determine the amplitude of the field transmitted through the second window:

$$\mathbf{E}_t(z, t) = \frac{1}{2}E_t \exp[-i(\omega t - kn_2z + \phi)] + \text{c.c.}, \quad (2)$$

[for convenience, one chooses $\phi = k(n_2 - 1)L$], and the amplitude of the reflected field that propagates back in the first window:

$$\mathbf{E}_r(z, t) = \frac{1}{2}E_r \exp[-i(\omega t + kn_1z)] + \text{c.c.} \quad (3)$$

Note that in Eqs. (1)–(3), E_{in} is assumed for simplicity to be real, while E_r and E_t are constant (propagation of a plane wave through a transparent window), but not necessarily real. Also, one may wish to calculate the resonant modifications E'_t (with $E''_t = E_t - E'_t$) and E'_r (with $E''_r = E_r - E'_r$) imposed on the transmitted and reflected field, respectively, with E'_t and E'_r the respective field amplitudes when the atomic medium is transparent (i.e., nonresonant). Let us recall that finding E'_t and E'_r is nothing other than solving the elementary problem of an empty FP cell.

To solve the problem, the two continuity equations for the electromagnetic fields at each interface are to be completed by the Maxwell equation for the propagation through the resonant medium. We describe in a formal manner the field inside the atomic medium by

$$\mathbf{E}_o(z, t) = \frac{1}{2}E_o(z) \exp[-i(\omega t - kz)] + \text{c.c.}, \quad (4)$$

and in a similar manner we take the polarization in the form

$$\mathbf{P}_o(z, t) = \frac{1}{2}P_o(z) \exp[-i(\omega t - kz)] + \text{c.c.} \quad (5)$$

Note that to deal with the possibility of a major inhomogeneity (along the z -direction) of the atomic response that may originate notably in the effects of nonlinear response (saturation, etc.), long-range atom–surface interaction, or transient effects associated with the atomic mo-

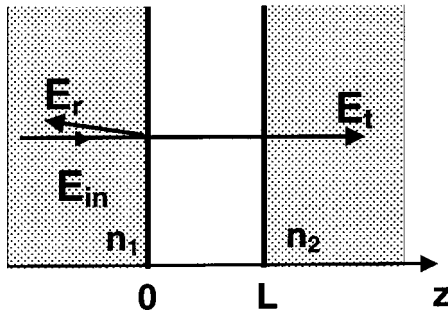


Fig. 1. Thin layer (thickness L) of a (resonant) atomic medium sandwiched between two parallel, transparent, dielectric windows with index of refraction n_1 for $z < 0$, and n_2 for $z > L$.

tion, we make no special assumption for the field structure inside the medium, i.e., for $E_o(z)$. Let us emphasize that we do not use here the slowly varying envelope—known to be inadequate to deal with SR problems^{12,13}—nor a local description with a complex index, as usual in thin-film optics.

Hence, we get from the electromagnetic continuity at the $z = 0$ boundary

$$E_{\text{in}} + E_r = E_o(0), \quad (6)$$

$$in_1k(E_{\text{in}} - E_r) = ikE_o(0) + \frac{\partial E_o}{\partial z}(0), \quad (7)$$

and at the $z = L$ boundary, we have

$$E_o(L) = E_t, \quad (8)$$

$$\left[ikE_o(L) + \frac{\partial E_o}{\partial z}(L) \right] = in_2kE_t. \quad (9)$$

Inside the resonant medium, the field must obey the Maxwell propagation equation, which simplifies to Eq. (10) under the assumptions that we neglect the conductivity losses in the media and that the excitation is stationary (cw excitation):

$$\frac{\partial^2 E_o(z)}{\partial z^2} + 2ik \frac{\partial E_o(z)}{\partial z} = -(k^2/\epsilon_o)P_o(z). \quad (10)$$

Eq. (10) can be converted to the equivalent form

$$\frac{\partial}{\partial z} \left[\exp(2ikz) \frac{\partial E_o(z)}{\partial z} \right] = -(k^2/\epsilon_o)P_o(z) \exp(2ikz). \quad (11)$$

Assuming the local atomic response $P_o(z)$ to be known (see Section 5 for a calculation in the case of a two-level dilute atomic system), the integration of Eqs. (10) and (11) from $z = 0$ to L provides the necessary coupling between the boundary equations (6), (7) and (8), (9). Indeed, one obtains

$$\frac{\partial E_o}{\partial z}(L) - \frac{\partial E_o}{\partial z}(0) + 2ik[E_o(L) - E_o(0)] = 2ikI_f, \quad (12)$$

$$\frac{\partial E_o}{\partial z}(L) \exp(2ikL) - \frac{\partial E_o}{\partial z}(0) = 2ikI_b. \quad (13)$$

In Eqs. (12) and (13), we have defined

$$I_f = ik/2\epsilon_o \int_0^L P_o(z) dz, \quad (14)$$

$$I_b = ik/2\epsilon_o \int_0^L P_o(z) \exp(2ikz) dz. \quad (15)$$

The solution of the linear system of six equations [(6)–(9) and (12), (13)] with respect to E_t and E_r is straightforward and naturally discriminates between the empty-FP solution E'_t and E'_r (as obtained with $P_o = 0$, i.e., $I_f = I_b = 0$) and the resonant contributions E''_t and E''_r , respectively. One gets

$$E'_t = t_{02}t_{10}E_{\text{in}}/F, \quad (16)$$

$$E'_r = [r_1 - r_2 \exp(2ikL)]E_{\text{in}}/F, \quad (17)$$

$$E''_t = t_{02}(I_f - r_1I_b)/F, \quad (18)$$

$$E''_r = t_{01}[I_b - r_2I_f \exp(i2kL)]/F. \quad (19)$$

In Eqs. (16)–(19), the following notations are used:

$$r_1 = \frac{n_1 - 1}{n_1 + 1}, \quad r_2 = \frac{n_2 - 1}{n_2 + 1},$$

$$t_{10} = \frac{2n_1}{n_1 + 1}, \quad t_{01} = \frac{2}{n_1 + 1},$$

$$t_{02} = \frac{2}{n_2 + 1},$$

and $F = 1 - r_1r_2 \exp(2ikL)$.

Equations (18) and (19) represent the major result of the present work. Indeed, the integrals I_f and I_b are known to be associated, respectively, with standard transmission spectroscopy and SR spectroscopy,^{1,12} in the limit of a long cell ($L \rightarrow \infty$). What is shown here is that the backward response I_b cannot be neglected in the transmission detection, even with an antireflection coating on the second window (in our model, this may be approached with $n_2 \rightarrow 1$, leading to $r_2 \rightarrow 0$ —for the extension to a multilayer window, see Ref. 14). The I_b contribution would vanish only for an antireflection-coated first window, a situation in which no reflection signal could be considered.¹⁵ In a very similar manner, in a reflection experiment, the forward response—usually associated with transmission—is always present (it cancels only for $r_2 = 0$), although it is modulated with a phase factor. Also, as a general result and from an optical point of view, the FP nature of the cell appears fully taken into account by the F factor, with no multiple interference between I_f and I_b . An additional but independent FP effect may have to be considered, however, in a detailed evaluation of the atomic response I_f and I_b : It relates to the spatial oscillation of the driving field $E_o(z)$, whose amplitude governs the medium response $P_o(z)$.

Note that in most approaches, the I_b contribution appearing in Eq. (18) has usually been neglected, and this is justified because, as opposed to the intrinsically phase-matched I_f response, the I_b response has a coherence length limited to an (reduced) optical wavelength [see Eq. (15)]: As long as the cell length significantly exceeds a wavelength, the I_b term is indeed much smaller than the I_f term. This I_b contribution has been mentioned only briefly in Ref. 5 [notably in its Eq. (9)], with no mention of the consequences for the line-shape symmetry. Conversely, with phase-matching arguments, one sees from Eq. (19) that, for relatively long cells of a dilute medium, I_f may even dominate the expected backward response I_b , provided the second window is not antireflection coated. This actually corroborates early experimental data.⁹

In many usual cases, the dilute character of the vapor implies $E''_r \ll E'_r$ and $E''_t \ll E'_t$. Hence, the respective resonant transmission and reflection contributions given

by $S_t = |E_t|^2 - |E'_t|^2$ and $S_r = |E_r|^2 - |E'_r|^2$ can be interpreted as a homodyne beating with the transmitted (reflected) field of an empty FP cell. One gets the simple expressions

$$S_t \approx 2t_{10}t_{02}^2E_{\text{in}} \operatorname{Re}(I_f - r_1I_b)/|F|^2, \quad (20)$$

$$S_r \approx 2t_{01}E_{\text{in}} \operatorname{Re}\{[r_1 - r_2 \exp(-2ikL)] \times [I_b - r_2I_f \exp(2ikL)]\}/|F|^2. \quad (21)$$

Note that for identical windows (i.e., $n_1 = n_2$ and $r_1 = r_2 = r$), the reflection signal from the empty FP cell vanishes ($E'_r = 0$; see Eq. 17) with a periodicity $\lambda/2$ when $L = m\lambda/2$ (with m =integer). In this special case, the measured reflected signal consists of the intensity of the signal re-emitted from the vapor only. The reflected signal, hence proportional to $|E''_r|^2$, is expected to exhibit much smaller amplitude along with line-shape peculiarities following

$$S_r = \frac{|I_b - rI_f|^2}{(1 + r)^2}. \quad (22)$$

3. DILUTE VAPOR AND THE OPTICALLY THIN-MEDIUM APPROXIMATION

The above general derivation leads to tractable calculation only when I_f and I_b can be evaluated.¹⁶ In the limit of a very dilute medium, which can be characterized by $E''_t \ll E'_t$, the field $E_o(z)$ that drives the polarization $P_o(z)$ in the medium is essentially the field $E'_o(z)$ of an empty FP [with $E_o(z) = E'_o(z) + E''_o(z)$ and the respective components $E'_o(z)$ and $E''_o(z)$ defined in the same manner as in Section 2 for the reflected and transmitted fields].

One has

$$E'_o(z) = E_{\text{in}}t_{10}\{1 - r_2 \exp[-2ik(z - L)]\}/F. \quad (23)$$

From Eq. (23), with the total E_o field given by Eq. (4), we see that E'_o always exhibits a node at the second window ($z = L$), while the partly standing-wave nature has the expected $\lambda/2$ FP periodicity. A specific feature of the thin vapor cell is that the contrast between nodes and antinodes rises to $(1 + r_2)/(1 - r_2) = n_2$, or to n_2^2 in intensity, and so can be rather large (e.g., several units). However, it usually remains a low-finesse FP, so that in spite of the local minima of $|E'_o(z)|$, the condition $|E''_o(z)| \ll |E'_o(z)|$ can usually be fulfilled throughout the cell as long as the assumption $E''_t \ll E'_t$ is valid. This spatial modulation is expected to imply heavy consequences on the structure of the dipole polarization induced in the medium, especially when combined with a spatially inhomogeneous response. Among examples sustained by present investigations in our laboratory, one may consider nonlinear processes such as a two-photon excitation, or processes possibly driven by auxiliary pump fields: Combined with the additional effect of the FP field structure affecting the pump fields, one may expect quick spatial variations for the induced polarization $P_o(z)$ and the corresponding field $E''_o(z)$. Also, when considering the influence of long-range van der Waals atom–surface interaction on the optical properties of the cell (a complete

analysis will be deferred to a subsequent publication), one predicts a smaller influence of the second window than would be expected without an analysis of the FP structure. Conversely, the driving field is maximized close to the first window when the cell length is an odd multiple of $\lambda/4$, and the sensitivity to atom–interaction with the first surface may be enhanced. It should be added that these effects, related to the spatial inhomogeneity of the driving field $E'_o(z)$, will usually be reduced when the atomic motion is considered to be the result of a spatial averaging.

4. LINEAR REGIME OF INTERACTION

As long as the resonant medium response behaves linearly with respect to the driving field, and as long as the optically thin-medium approximation is satisfied (see Section 3), one may write

$$E'_o = \frac{1}{2}E_o^{+'} \exp[-i(\omega t - kz)] + \frac{1}{2}E_o^{-'} \exp[-i(\omega t + kz)] + \text{c.c.}, \quad (24)$$

$$P_o = \frac{1}{2}P_o^+(z)\exp[-i(\omega t - kz)] + \frac{1}{2}P_o^-(z)\exp[-i(\omega t + kz)] + \text{c.c.}, \quad (25)$$

with $P_o^+(z)$ and $P_o^-(z)$ driven only by the respective forward and backward field amplitudes $E_o^{+'}$ and $E_o^{-'}$. In Eq. (24), we have taken, according to Eqs. (23) and (4),

$$E_o^{+'} = E_{\text{int}10}/F \quad (26)$$

$$E_o^{-'} = -E_{\text{int}10}r_2 \exp(2ikL)/F \\ = -r_2 \exp(2ikL)E_o^{+'}, \quad (27)$$

and one gets from Eq. (5)

$$P_o(z) = P_o^+(z) + P_o^-(z)\exp(-2ikz). \quad (28)$$

Within the approximation of an interaction that is linear with the driving field, such an expression permits us to use the numerous studies (see, e.g., Refs. 2–9, 12, 13, 17–23) that assume a traveling-wave excitation with a constant amplitude (i.e. optically thin medium), as can be found in the literature devoted to transmission spectroscopy and SR spectroscopy. Moreover, with some assumptions of symmetry between the two windows that are quite common (notably, the symmetry of the velocity distribution, an identical surface interaction exerted by the two windows, and a spatial homogeneity—or a symmetry—of the extra-pumping effects when they are allowed by the model), one finds that

$$\frac{P_o^-(L-z)}{E_o^{-'}} = \frac{P_o^+(z)}{E_o^{+'}}. \quad (29)$$

Combining Eqs (26) and (27) with (14) and (15), one can express the resonant contribution to the transmitted and reflected fields [Eqs. (18) and (19)] as a combination of the common transmission and SR signals,²⁴ as calculated with only one traveling-wave excitation and neglecting internal reflections inside the cell. These transmission and reflection signals are known to be governed, respectively,

$$I_T^{\text{lin}} = ik/2\varepsilon_o \int_0^L P_o^+(z) dz, \quad (30)$$

$$I_{\text{SR}}^{\text{lin}} = ik/2\varepsilon_o \int_0^L P_o^+(z) \exp(2ikz) dz. \quad (31)$$

Then Eqs. (14) and (15) can be written [using Eqs. (27)–(31)]

$$I_f = I_T^{\text{lin}} - r_2 I_{\text{SR}}^{\text{lin}}, \quad (32)$$

$$I_b = I_{\text{SR}}^{\text{lin}} - r_2 \exp(2ikL) I_T^{\text{lin}}. \quad (33)$$

The thin-cell transmission depends on [Eqs. (18) and (19)]

$$I_T = I_f - r_1 I_b = [1 + r_1 r_2 \exp(2ikL)] I_T^{\text{lin}} \\ - [r_1 + r_2] I_{\text{SR}}^{\text{lin}}, \quad (34)$$

while the thin-cell reflection depends on

$$I_{\text{SR}} = I_b - r_2 I_f \exp(2ikL) \\ = [1 + r_2^2 \exp(2ikL)] I_{\text{SR}}^{\text{lin}} - 2[r_2 \exp(2ikL)] I_T^{\text{lin}}. \quad (35)$$

In spite of the few simplifying assumptions that we have made, we have obtained with Eqs. (34) and (35) the expressions showing how thin-cell spectroscopy combines interferometrically responses and line shapes that are known otherwise. In Section 5, these results are illustrated in the elementary case of a Doppler-broadened, two-level medium for which extensive solutions have been already given in Refs. 4, 5, and 7, and in Refs. 8 and 9 in the case of the FM regime at the large-Doppler limit.

5. DILUTE TWO-LEVEL MEDIUM IN THE LINEAR REGIME

The case of a resonant Doppler-broadened, two-level medium has been considered extensively.^{4,5,7} Under the following assumptions:

1. The vapor is dilute enough that only atom–surface collisions are to be considered,
2. atoms leave the wall in the ground state,
3. the incident laser beam diameter largely exceeds the cell thickness,

one derives the following line shape from a spatial integration of the transient atomic response:

$$I_T^{\text{lin}} = C \int_{-\infty}^{+\infty} W(v) g(\omega - \omega_o, v, L) dv, \quad (36)$$

$$I_{\text{SR}}^{\text{lin}} = C \int_{-\infty}^{+\infty} W(v) h(\omega - \omega_o, v, L) dv, \quad (37)$$

with⁷

$$g(\omega - \omega_o, v, L) = -\frac{k}{\Lambda_+} \left\{ L - \frac{|v|}{\Lambda_+} \right. \\ \left. \times \left[1 - \exp\left(-\frac{\Lambda_+ L}{|v|} \right) \right] \right\}, \quad (38)$$

$$\Lambda_{\pm} = \gamma - i(\omega - \omega_o) \pm ikv, \quad (39)$$

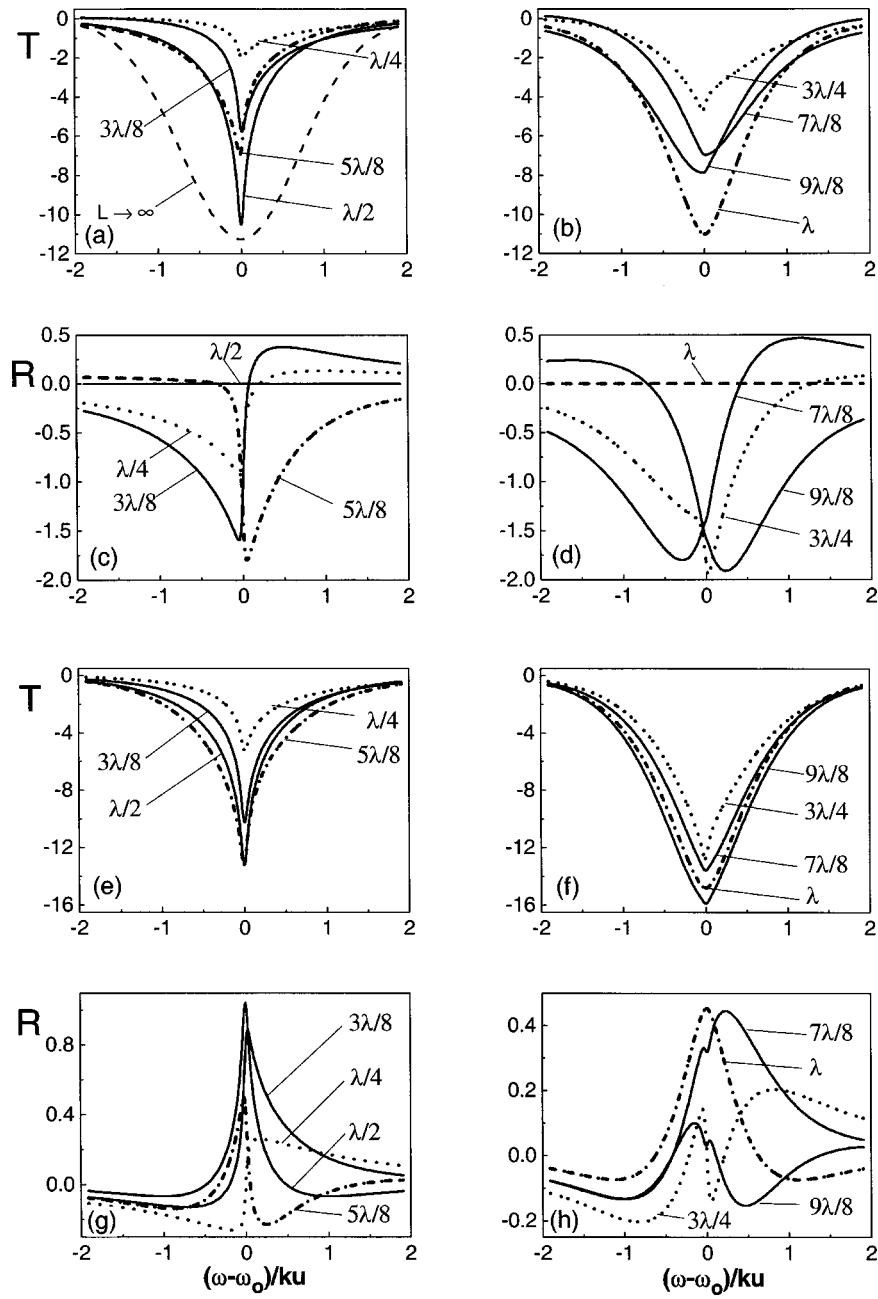


Fig. 2. Theoretical line shapes for a two-level system in the linear regime as evaluated for various cell lengths (as indicated): the T values for (a), (b), (e), (f) and R values for (c), (d), (g), (h) correspond to the respective resonant modifications of the transmitted amplitude and of the reflected amplitude. These values naturally account for the FP resonance through the F factor appearing in Eqs. (20) and (21) and coefficient C . For purposes of comparison, a single vertical scale (in arbitrary units) has been used. The various line shapes permit one to compare, respectively, a cell with two identical windows [(a)–(d) with $r_1 = r_2 = 0.29$] and a cell whose output window has an antireflection coating [(e)–(h) with $r_1 = 0.29, r_2 = 0$]. The spectra are calculated with $\gamma/ku = 0.025$. It is recalled that in a macroscopic cell, the transmission linewidth is an absorption Voigt profile that can be approximated, as long as $\gamma \ll ku$, by the Gaussian line shape represented in (a) by the dashed curve for $L \rightarrow \infty$ (arbitrary vertical scale, half-width at $1/e : ku$).

$$\begin{aligned}
 h(\omega - \omega_0, v, L) &= h_{\pm}(\omega - \omega_0, v, L) \\
 &= \frac{1}{2i} \left[\frac{1}{\Lambda_{\mp}} - \frac{\exp(2ikL)}{\Lambda_{\pm}} \right] \\
 &\quad - \frac{k|v|}{\Lambda_+ \Lambda_-} \exp\left(-\frac{\Lambda_{\mp} L}{|v|}\right). \quad (40)
 \end{aligned}$$

In Eqs. (36)–(40), we have used the following notations: ω_0 and γ define the atom transition frequency and optical

width, respectively; k is the wave vector modulus; $W(v)$ stands for the normalized distribution of the normal velocity component; $h_{\pm}(v)$ are chosen, respectively, for $v > 0$ and $v < 0$ in Eq. (40), and C is a constant depending on the atomic density N and the transition dipole moment μ , where

$$C = \frac{N\mu^2 t_{10} E_{in}}{4\hbar F \epsilon_0}. \quad (41)$$

With the standard assumption of a Maxwellian velocity distribution $W(v) = (u\sqrt{\pi})^{-1} \exp(-v^2/u^2)$, with $u \equiv$ the thermal velocity, I_T^{lin} and $I_{\text{SR}}^{\text{lin}}$ exhibit some special symmetry properties depending on the cell length L (modulo the wavelength λ), along with a sub-Doppler structure superimposed on Doppler-broadened wings. A discussion of these symmetry properties of $I_{\text{SR}}^{\text{lin}}$ and I_T^{lin} was given in Ref. 5, although the range of L values considered there was too limited to cover the full range of the pseudo-period λ of the atomic response.

Figure 2 illustrates the theoretically predicted transmission [Fig. 2(a) and (b) and Fig. 2(e) and (f)] and reflection [Fig. 2(c) and (d) and Fig. 2(g) and (h)] spectra as determined by applying Eqs. (36) and (37) to Eqs. (34) and (35) and exporting them to Eqs. (20) and (21), corresponding to a realistic ultrathin cell. As is known from Eqs. (36) and (37), and as a major interest of thin-cell spectroscopy, the spectra clearly exhibit sub-Doppler components related to the enhanced contribution of atoms undergoing a long interaction time. Different cell lengths are considered, and the results permit a comparison between a symmetric ultrathin cell [assuming $r_1 = r_2 = 0.29$, a typical value for a YAG window; see Figs. 2(a)–2(d)] and a cell with $r_1 = 0.29$ and $r_2 = 0$ [see Figs. 2(e)–2(h)] whose output window would ideally be antireflection coated as in Refs. 4 and 5, hence eliminating the FP structure of the driving field. In all cases, the overall spectra exhibit sub-Doppler features that are specially marked when the thickness is close to $\lambda/2, 3\lambda/2, \dots$, and this enhancement of the sub-Doppler structure is a transient coherent response property of the interaction buildup between walls, as first noted in Ref. 25. One also notices in all cases that the transmission spectrum is no longer a simple absorption spectrum, nor a symmetric spectrum solely connected with absorption properties, as was predicted when internal reflection on the input window was neglected (i.e., $r_1 = 0$).^{4,5} Rather, it includes a dispersive contribution related to the mixing between absorption-spectrum line shape and selective reflection line shape as given by

$I_T = I_T^{\text{lin}} - r_1 I_{\text{SR}}^{\text{lin}}$. As far as the SR spectrum is concerned, one first notes that in all cases, it becomes hard to reproduce the familiar dispersion-like properties of the selective reflection in a long cell.²⁶ With an antireflection coating on the output window, the SR spectra [Fig. 2(g)–(h)], depending only on the SR term $I_{\text{SR}} = I_{\text{SR}}^{\text{lin}}$, actually reproduce the spectra reported in Refs. 4 and 5 with its occasional symmetry properties (symmetric line shape for $L = m\lambda/2$, antisymmetric ones for $L = (2m + 1)\lambda/4$, $m \equiv$ integer). For a cell with identical windows, the spectra no longer exhibit any recognizable symmetry, and the differences with an antireflection-coated cell get stronger with increasing cell length, as the contribution of the essentially absorption-like I_T gets relatively larger. Note also that the resonant reflection signal for $L = \lambda/2, \lambda, 3\lambda/2, 2\lambda, \dots$, is too small to be seen, as expected with a symmetric FP [see discussion in Section 2 and see Eq. (22)]. In a similar manner, the increase in the transmitted field apparently predicted in the far wings of the spectra [see, e.g., the red wing for $L = 7\lambda/8$ and the blue wing for $L = 9\lambda/8$ in Fig. 2(b)] simply relates to a shift in the FP resonance induced by the vapor dispersion that dominates in the wings of the resonance.

6. FREQUENCY-MODULATED SPECTROSCOPY WITH A TWO-LEVEL SYSTEM

It can also be convenient to consider the FM version of thin-cell spectroscopy, because in the Doppler limit, and for a two-level system in the linear regime as considered in Section 5, the FM spectrum—obtained as the frequency derivative of the spectrum assuming a low-index modulation—can be evaluated through an analytical velocity integration.^{8,17,27} In particular, while it is known that the analytical evaluation of I_T^{lin} and of $I_{\text{SR}}^{\text{lin}}$ leads, in the Doppler limit, to a logarithmic divergence of a sub-Doppler structure associated with the enhanced transient

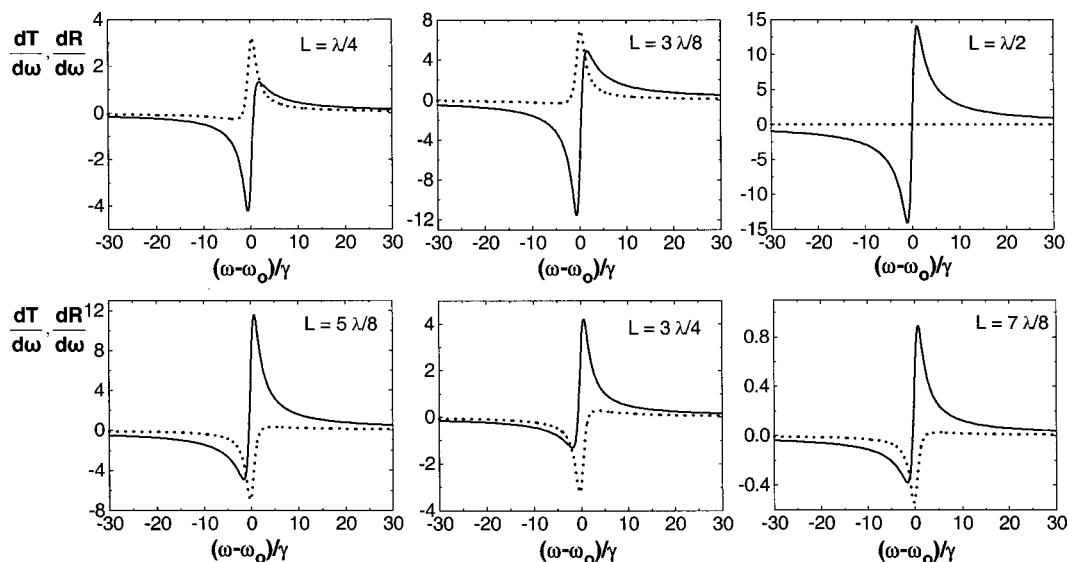


Fig. 3. Theoretical transmission $dT/d\omega$ (solid curve) and reflection $dR/d\omega$ (dashed curve) spectra in the FM regime for different cell lengths as indicated, assuming two identical windows ($r_1 = r_2 = 0.29$). A single vertical scale has been used, and the signal amplitudes account for the FP resonance through the F factor appearing in Eqs. (47) and (48) and coefficient C.

contribution of slow atoms, the corresponding FM line shapes are purely Doppler-free, as is well known in SR spectroscopy in a macroscopic cell.^{17,27} The FM approach also corresponds to experimental situations of major interest as being due to a notable enhancement of the narrow structure.^{6–10,27}

Extending the calculation described in Ref. 17 that starts from standard Bloch equations to the case of a cell of a finite length, one gets, assuming that the cell is short enough ($L \ll u/\gamma$), the (FM) local induced polarization after a velocity integration in the Doppler limit (i.e., $ku \gg \gamma$):

$$\frac{dP_o^+}{d\omega}(z) = 2\varepsilon_o C \frac{[\exp(ikL - ikz) - \exp(-ikz)]}{[\gamma - i(\omega - \omega_o)]ku\sqrt{\pi}}, \quad (42)$$

with C defined in Eq. (41). From this simple Lorentzian shape of the (FM) induced polarization as calculated with a single traveling wave, one easily deduces with Eqs. (30) and (31)

$$\frac{dI_T^{\text{lin}}}{d\omega} = -\frac{4i}{ku\sqrt{\pi}} C \frac{\sin^2(kL/2)}{\gamma - i(\omega - \omega_o)}, \quad (43)$$

$$\frac{dI_{\text{SR}}^{\text{lin}}}{d\omega} = \frac{dI_T^{\text{lin}}}{d\omega} \exp(ikL). \quad (44)$$

Exporting Eqs. (43) and (44) into Eqs. (34) and (35) that account for the FP effects, and considering for simplicity the symmetric cell with $r_1 = r_2 = r$, one obtains

$$\begin{aligned} \frac{dI_T}{d\omega} &= -\frac{4i}{ku\sqrt{\pi}} C [1 - r \exp(ikL)]^2 \\ &\times \frac{\sin^2(kL/2)}{\gamma - i(\omega - \omega_o)}, \end{aligned} \quad (45)$$

along with a relation analogous to Eq. (44):

$$\frac{dI_{\text{SR}}}{d\omega} = \frac{dI_T}{d\omega} \exp(ikL). \quad (46)$$

It should be noted that this general result shows that, inside the vapor, the FM amplitude governing the transmission signal is equal (in modulus) to that relevant for the SR signal. This is obtained whatever the reflection coefficient of the windows, although the measured transmission and SR signals have a different size depending on r , notably through the F factor. Note also that Eqs. (45) and (46) imply a simultaneous periodic vanishing of the FM signals for $L = m\lambda$, corroborating the disappearance of the narrow sub-Doppler contribution appearing in Fig. 2 for these cell thicknesses.

Finally, the respective FM signals (with the interference taken into account) in forward and backward directions are given by the simple expressions:

$$\frac{dS_t}{d\omega} = \frac{2(1-r)(1-r^2)E_{\text{in}}}{|F|^2} \text{Re}\left(\frac{dI_T}{d\omega}\right), \quad (47)$$

$$\frac{dS_r}{d\omega} = -\frac{4(1-r)rE_{\text{in}} \sin(kL)}{|F|^2} \text{Im}\left(\frac{dI_T}{d\omega}\right). \quad (48)$$

Figure 3 illustrates the results of Eqs. (47) and (48). The FM technique that eliminates the Doppler wings finally yields, for both signals, a complex admixture of absorptive and dispersive Lorentzians. Note also that in the limit of two antireflection windows ($r_1 = r_2 = r \rightarrow 0$), Eq. (47) generalizes the line shape and length dependence that has been mentioned previously (see footnote 18 in Ref. 8).

7. CONCLUSION

In conclusion, we have shown that for very thin vapor cells, and especially when the cell thickness L is smaller than the optical wavelength or comparable with it, the measured transmission and reflection are strongly dependent on the intrinsic FP nature of the thin cell. In this dependence, we have distinguished, in the general approach considered here, the effects related to the partly standing-wave nature of the irradiating field and the effects associated with the details of the propagation (forward, but also backward) of the field resulting from the induced dipole polarization. In the case of a two-level system in the linear regime, experiments have recently been performed in our group, notably on the cesium D_1 line, and will be reported elsewhere.²⁸ The correct analysis of the various effects associated with the FP nature of the thin cell is of high importance in any attempt to extract information on the atom-surface interaction potential from extremely thin-cell spectroscopy. Such an atom-surface interaction is presently observed in experiments in progress that are based on a nonlinear spectroscopy scheme for transitions between excited states, and the interaction appears to induce huge shifts for subwavelength cell thickness. Finally, we should mention that the general theoretical method used in the present paper should be of interest in extending the treatment to a vapor located between two prisms, where total reflection can undergo a frequency-dependent frustration.

ACKNOWLEDGMENT

Work was partially supported in the frame of the FAST-Net programme (European contract HPRN-CT-2002-00304).

S. Satiel's permanent address is University of Sofia, Department of Physics, Sofia, Bulgaria; e-mail satiel@phys.uni-sofia.bg.

The e-mail address of D. Bloch (corresponding author) is bloch@lpl.univ-paris13.fr.

REFERENCES AND NOTES

1. M. F. H. Schuurmans, "Spectral narrowing of selective reflection," *J. Phys. (Paris)* **37**, 469–485 (1976).
2. A. Ch. Izmailov, "On the possibility of sub-Doppler structure of spectral lines of gas particles by a single travelling monochromatic wave," *Laser Phys.* **2**, 762–763 (1992).
3. A. Ch. Izmailov, "Manifestations of sub-Doppler structure of the spectral lines of gas particles in the radiation of a travelling monochromatic pump wave," *Opt. Spektrosk.* **74**, 41–48 (1993) [*Opt. Spectrosc.* **74**, 25–29 (1993)].
4. T. A. Vartanyan and D. L. Lin, "Enhanced selective reflection from a thin layer of a dilute gaseous medium," *Phys. Rev. A* **51**, 1959–1964 (1995).

5. B. Zambon and G. Nienhuis, "Reflection and transmission of light by thin vapor layers," *Opt. Commun.* **143**, 308–314 (1997).
6. S. Briaudeau, D. Bloch, and M. Ducloy, "Detection of slow atoms in laser spectroscopy of a thin vapor film," *Europhys. Lett.* **35**, 337–342 (1996).
7. S. Briaudeau, S. Saltiel, G. Nienhuis, D. Bloch, and M. Ducloy, "Coherent Doppler narrowing in a thin vapor cell: Observation of the Dicke regime in the optical domain," *Phys. Rev. A* **57**, R3169–3172 (1998).
8. S. Briaudeau, D. Bloch, and M. Ducloy, "Sub-Doppler spectroscopy in a thin film of resonant vapor," *Phys. Rev. A* **59**, 3723–3735 (1999).
9. S. Briaudeau, "Spectroscopie à haute résolution en vapeur confinée," thèse de doctorat, Laboratoire de Physique des Lasers, Université Paris 13 (1998) (unpublished).
10. S. Briaudeau, S. Saltiel, J. R. R. Leite, M. Oria, A. Bramati, A. Weis, D. Bloch, and M. Ducloy, "Recent developments in sub-Doppler spectroscopy in a thin cell," *J. Phys. IV* **10**, Pr. 8, 145–146 (2000).
11. D. Sarkisyan, D. Bloch, A. Papoyan, and M. Ducloy, "Sub-Doppler spectroscopy by sub-micron thin Cs-vapor layer," *Opt. Commun.* **200**, 201–208 (2001).
12. G. Nienhuis, F. Schuller, and M. Ducloy, "Nonlinear selective reflection from an atomic vapor at arbitrary incidence angle," *Phys. Rev. A* **38**, 5197–5205 (1988).
13. F. Schuller, G. Nienhuis, and M. Ducloy, "Selective reflection from an atomic vapor in a pump-probe scheme," *Phys. Rev. A* **43**, 443–454 (1991).
14. M. Chevrollier, M. Oria, J. G. De Souza, D. Bloch, M. Fichet, and M. Ducloy, "Selective reflection spectroscopy of a resonant vapor at the interface with a metallic layer," *Phys. Rev. E* **63**, 046610 (2001).
15. Note that r_1 is an amplitude reflection coefficient usually not much smaller than unity; in recent experiments (see Ref. 11) performed with a narrow cell with yttrium aluminum garnet (YAG) windows, one has $n_1 = 1.82$, i.e., $r_1 = 0.29$. Note also that even with an antireflection coating, one usually has $r_{1,2} \geq 0.1$.
16. The difficulties typical of the optically thick medium in comparable problems have been analysed in the appendix of Ref. 1 and in T. Vartanyan, D. Bloch, and M. Ducloy, "Blue shift paradox in selective reflection," in *Spectral Line Shapes*, A. D. May, J. R. Drummond, eds., AIP Conference Proceedings **328** (American Institute of Physics, New York, 1995), pp. 249–250.
17. M. Ducloy and M. Fichet, "General theory of frequency modulated selective reflection. Influence of atom surface interactions," *J. Phys. II* **1**, 1429–1446 (1991).
18. F. Schuller, O. Gorceix, and M. Ducloy, "Nonlinear selective reflection in cascade three-level atomic systems," *Phys. Rev. A* **47**, 519–528 (1993).
19. G. Nienhuis and F. Schuller, "Selective reflection from a vapor of three-level atoms," *Phys. Rev. A* **50**, 1586–1592 (1994).
20. M. Gorris-Neveux, P. Monnot, S. Saltiel, R. Barbé, J. C. Keller, and M. Ducloy, "Two-photon selective reflection," *Phys. Rev. A* **54**, 3386–3393 (1996).
21. F. Schuller, A. Amy-Klein, and S. Saltiel, "Saturation effects in three-level selective reflection," *Phys. Rev. A* **53**, 3647–3651 (1996).
22. H. van Kampen, V. A. Sautenkov, E. R. Eliel, and J. P. Woerdman, "Probing the spatial dispersion in a dense atomic vapor near a dielectric interface," *Phys. Rev. A* **58**, 4473–4478 (1998).
23. D. Petrosyan and Yu. P. Malakyan, "Electromagnetically induced transparency in a thin vapor film," *Phys. Rev. A* **61**, 053820 (2000).
24. Note that the restriction to a finite cell length may introduce some additional changes relative to most common SR theories, as elaborated for various atomic models.
25. R. H. Romer and R. H. Dicke, "New technique of high-resolution microwave spectroscopy," *Phys. Rev.* **99**, 532–536 (1955).
26. The essential dispersive response of SR spectroscopy in a long cell results only from the SR spatial averaging, which washes out the atomic response close to the (remote) second window. It should be recalled also that because of the symmetry breakdown occurring between arriving and departing atoms, and because of the atom–surface interaction, SR spectra in a long cell commonly include, in the vicinity of line center, a mixture of absorptive and dispersive responses—see notably the discussions in M. Chevrollier, M. Fichet, M. Oria, G. Rahmat, D. Bloch, and M. Ducloy, "High resolution selective reflection spectroscopy as a probe of long-range surface interaction: measurement of the surface van der Waals attraction exerted on excited Cs atoms," *J. Phys. II* **2**, 631–657 (1992); conversely, and as noted in Section 3 herein, the transmission through a relatively long cell exhibits simply absorption-like properties as long as the medium remains optically thin.
27. A. M. Akul'shin, V. L. Velichanskii, A. S. Zibrov, V. V. Nikitin, V. A. Sautenkov, E. K. Yurkin, and N. V. Senkov, "Collisional broadening of intra-Doppler resonances of selective reflection of the D_2 of cesium," *JETP Lett.* **36**, 303–306 (1982).
28. G. Dutier, A. Yarovitski, S. Saltiel, A. Papoyan, D. Sarkisyan, D. Bloch, and M. Ducloy, "Collapse and revival of a Dicke-type coherent narrowing in a sub-micron thick vapor cell transmission spectroscopy," *Europhys. Lett.* (to be published).